Simple Expression for Estimating the Switch Peak Voltage on the Class-E Amplifier With Finite DC-Feed Inductance

Arturo Fajardo Jaimes [1,2], Fernando Rangel de Sousa [1]

1- Radiofrequency Laboratory| Department of Electrical and Electronics Engineering | UFSC | Florianpolis, Brazil

2- Department of Electronics Engineering | Pontifical Xavierian University (PUJ) | Bogota, Colombia

UNIVERSIDADE FEDERAL
DE SANTA CATARINA

Table of Content

WBANs for what?

Observation 1

The world population is growing fast, from 1950 to 2010 the population increased by around 4,390,405,000 individuals [1].

WBANs for what?

Observation 1

The world population is growing fast, from 1950 to 2010 the population increased by around 4,390,405,000 individuals [1].

Observation 2

The human life expectancy has increased too, in the same period, the elderly population (60 years old or older) augmented by about 410,647,596 individuals, representing a change from 8% to 11.1% on the composition of the population [1]

WBANs for what?

Observation 1

The world population is growing fast, from 1950 to 2010 the population increased by around 4,390,405,000 individuals [1].

Observation 2

The human life expectancy has increased too, in the same period, the elderly population (60 years old or older) augmented by about 410,647,596 individuals, representing a change from 8% to 11.1% on the composition of the population [1]

Observation 3

Millions of people develop chronic or fatal diseases every year and around 80% of health-care system spending is on chronic condition management [2].

WBANs for what?

Observation 1

The world population is growing fast, from 1950 to 2010 the population increased by around 4,390,405,000 individuals [1].

Observation 2

The human life expectancy has increased too, in the same period, the elderly population (60 years old or older) augmented by about 410,647,596 individuals, representing a change from 8% to 11.1% on the composition of the population [1]

Observation 3

Millions of people develop chronic or fatal diseases every year and around 80% of health-care system spending is on chronic condition management [2].

Future health systems need to change the current medical care paradigms. If the system DOES NOT change, it will collapse.

WBANs means?

- In order to achieve health-care systems connected at person level, at least a network which can be wearable, or implanted in the human body is needed [3].

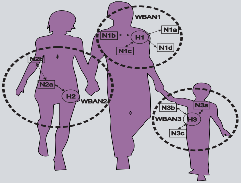

WBAN

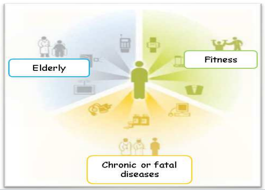

WBANs means?

- In order to achieve health-care systems connected at person level, at least a network which can be wearable, or implanted in the human body is needed [3].
- Networking at human body level without conscious intervention of the person. WBANs are expected to cause a dramatic shift in how people behave, in the same way the internet did. However, technical and social challenges must be faced before a natural adoption [3].

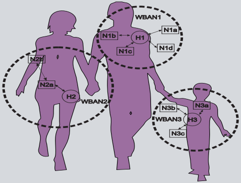

WBAN

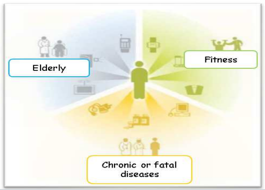

WPTn concept for implanted device autonomy

A WBAN node transfers energy to implanted device and receives information from it. In order to achieve energy autonomy, the WBAN node harvests energy from the body environment (i.e. solar and thermal). This energy is transferred through an inductive link (IL) to the passive implanted device that answers with the biomedical data.

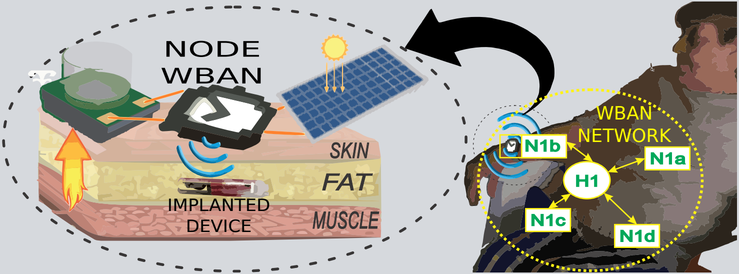

WPTn system view

- The IL uses the magnetic coupling between two inductors.

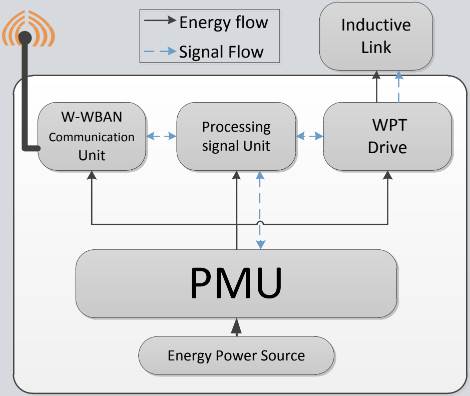

WPTn system view

- The IL uses the magnetic coupling between two inductors.
- The IL is expected to operate under weak coupling, therefore the WPT drive load is an inductive impedance with high Q value.

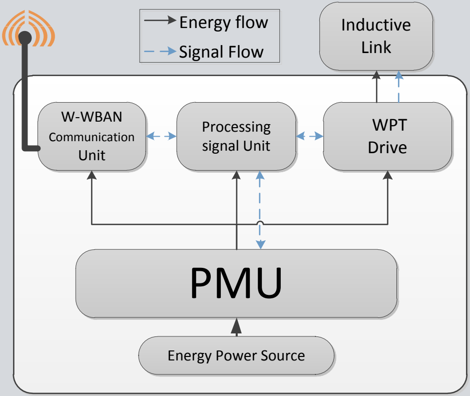

WPTn system view

- The IL uses the magnetic coupling between two inductors.
- The IL is expected to operate under weak coupling, therefore the WPT drive load is an inductive impedance with high Q value.
- The energy power source (EPS) is composed by the primary energy source (e.g. solar or thermal) and the harvester (e.g. photovoltaic cell or thermoelectric generator), and has a low power density.

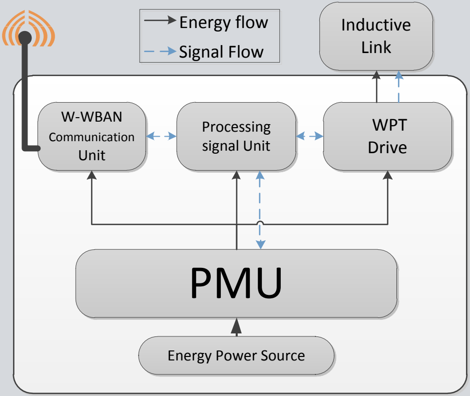

WPTn system view

- The IL uses the magnetic coupling between two inductors.
- The IL is expected to operate under weak coupling, therefore the WPT drive load is an inductive impedance with high Q value.
- The energy power source (EPS) is composed by the primary energy source (e.g. solar or thermal) and the harvester (e.g. photovoltaic cell or thermoelectric generator), and has a low power density.
- Given this EPS constrains, the efficiency of the WTP system (WTP Drive and IL) must be high in order to power the implanted node [4].

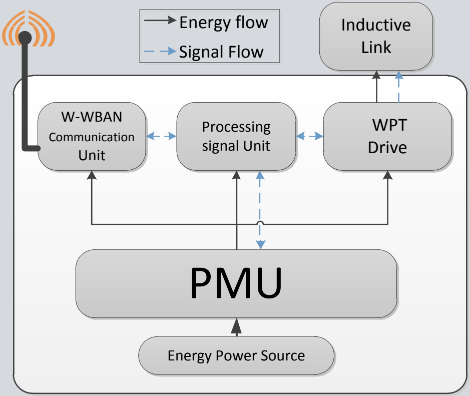

WPT driver

- One common implementation of the WPT driver (DC/RF converter) is an oscillator that drives a switched PA [5, 6, 7, 8].

WPT driver

- One common implementation of the WPT driver (DC/RF converter) is an oscillator that drives a switched PA [5, 6, 7, 8].
- Integrating a switched PA in a CMOS system-on-chip (SOC) is challenging, mainly due to the low breakdown voltage of CMOS devices and the low quality factor (Q) of the integrated passive components.

WPT driver

- One common implementation of the WPT driver (DC/RF converter) is an oscillator that drives a switched PA [5, 6, 7, 8].
- Integrating a switched PA in a CMOS system-on-chip (SOC) is challenging, mainly due to the low breakdown voltage of CMOS devices and the low quality factor (Q) of the integrated passive components.
- The published design methodologies for nominal or optimum operation of the class-E PA, that consider the switch breakdown voltage (i.e. a limit of the maximum switch voltage V_{S_M}) involves hard simulation work [9] or numerical method solution of non-linear equations [10].

WPT driver

- One common implementation of the WPT driver (DC/RF converter) is an oscillator that drives a switched PA [5, 6, 7, 8].
- Integrating a switched PA in a CMOS system-on-chip (SOC) is challenging, mainly due to the low breakdown voltage of CMOS devices and the low quality factor (Q) of the integrated passive components.
- The published design methodologies for nominal or optimum operation of the class-E PA, that consider the switch breakdown voltage (i.e. a limit of the maximum switch voltage V_{S_M}) involves hard simulation work [9] or numerical method solution of non-linear equations [10].
- In [11], the V_{S_M} was included in an analytical design set, it was divided in specification gains and circuit element gains as is illustrated in the figure.

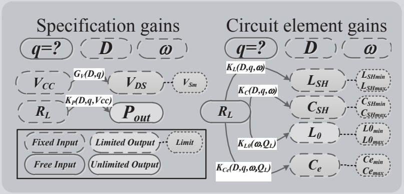

WPT driver

All of these gains are analytic functions of the input variables, therefore the design set can be implemented and calculated in any math software for analyzing all the involved trade-offs.

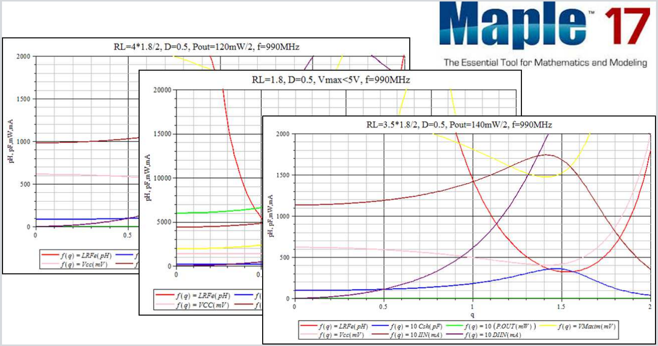

About this work

This work presents the synthesis of an analytic relationship between the DC input voltage and the peak switch voltage on an ideal class-E PA with finite dc-feed inductance, at zero voltage and zero slope of the switch voltage operation.

$$G_{Va}\left(D, q = \frac{1}{\omega\sqrt{L_{SH}C_{SH}}} = \frac{\omega_{SH}}{\omega}\right) = \frac{V_{S_M}}{V_{CC}} = \frac{1.8208}{1 - D}$$

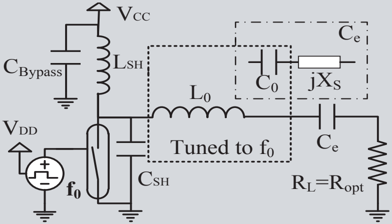

Class-E model [12] I

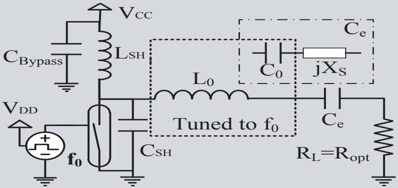

(a) Ideal model

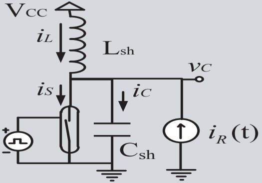

(b) Model High Q

$$i_R(t) = I_P sin\left(\omega t + \varphi\right) = \sqrt{\frac{2P_{OUT}}{R_L}} sin\left(2\pi f t + \varphi\right)$$

Class-E model [12] II

$$v_{C_{SH\,on}}(t) = i_{S_{off}}(t) = i_{C_{SH\,on}}(t) = 0$$

$$i_{L_{SH\,on}}(t) = \frac{V_{CC}}{L_{SH}} t - I_P sin(\varphi)$$

$$i_{S_{on}}(t) = \frac{V_{CC}}{L_{SH}} t + I_P \left(sin(\omega t + \varphi) - sin(\varphi)\right)$$

$$i_{C_{SH\,off}}(t) = \begin{array}{l} \frac{V_{CC}}{L_{SH}} t - \frac{1}{L_{SH}} \int_{\frac{2\pi D}{\omega}}^{t} v_{C_{SH}}(\tau) d\tau \\ + I_P \left(sin(\omega t + \varphi) - sin(\varphi)\right) \end{array}$$

$$i_{L_{SH\,off}}(t) = \frac{V_{CC}}{L_{SH}} t - \frac{1}{L_{SH}} \int_{\frac{2\pi D}{\omega}}^{t} v_{C_{SH}}(\tau) d\tau - I_P sin(\varphi)$$

Class-E model [12] III

$$v_{C_{SH\,off}}(t) = \begin{array}{c} V_{\mathrm{CC}} + C_1\cos(q\omega t) + C_2\sin(q\omega t) \\ -\frac{q^2}{1-q^2} p V_{\mathrm{CC}}\cos(\omega t + \varphi) \end{array}$$

$$C_1 = V_{\mathrm{DD}}\left\{ p\left(\begin{array}{c} \frac{q^2}{1-q^2}\cos(2q\pi)\cos(\varphi) \\ +\frac{q}{1-q^2}\sin(2q\pi)\sin(\varphi) \end{array} \right) - \cos(2q\pi) \right\}$$

$$C_2 = V_{\mathrm{DD}}\left\{ p\left(\begin{array}{c} \frac{q^2}{1-q^2}\sin(2q\pi)\cos(\varphi) \\ -\frac{q}{1-q^2}\cos(2q\pi)\sin(\varphi) \end{array} \right) - \sin(2q\pi) \right\}$$

$$q = \frac{1}{\omega\sqrt{L_{SH}C_{SH}}} = \frac{\omega_{SH}}{\omega};\ p = \frac{\omega L_{SH} I_P}{V_{CC}} = \frac{Z_{L_{SH}}}{R_\omega};$$

Limits of the models

Observation 1

It is important to emphasize that the model expressions can be calculated in terms of V_{CC}, ω, R_L, and P_{OUT} only if p,q,φ and D are known, but in [12] was demonstrated that both φ and p could be solved as a analytic function of both q and D.

Limits of the models

Observation 1

It is important to emphasize that the model expressions can be calculated in terms of V_{CC}, ω, R_L, and P_{OUT} only if p,q,φ and D are known, but in [12] was demonstrated that both φ and p could be solved as a analytic function of both q and D.

Observation 2

The model is valid when the control signals have 0 time transitions at a frequency f (near to f_0) and the series resonant circuit L_0, C_e and R_L has a high loaded quality factor.

Class-E Maximum switch voltage

The peak value of the switch voltage occurs when:

$$\frac{d}{dt} V_{C_{SH}}(\theta_m = \omega t_{max}) = 0;$$

Class-E Maximum switch voltage

The peak value of the switch voltage occurs when:

$$\frac{d}{dt} V_{C_{SH}}(\theta_m = \omega t_{max}) = 0;$$

Therefore θ_m can be calculated by:

$$\begin{aligned}
0 =\ & \cos(q\theta_m)\sin(2\pi q)\cos(\varphi)\,pq^2 - \cos(2\pi q)\sin(q\theta_m)\cos(\varphi)\,pq^2 \\
& - \sin(2\pi q)\sin(q\theta_m)\sin(\varphi)\,pq + \cos(q\theta_m)\sin(2\pi q)\,q^2 \\
& + pq\sin(\theta_m + \varphi) - \cos(q\theta_m)\sin(2\pi q) + \cos(2\pi q)\sin(q\theta_m) \\
& - \cos(q\theta_m)\cos(2\pi q)\sin(\varphi)\,pq - \cos(2\pi q)\sin(q\theta_m)\,q^2
\end{aligned}$$

Solving numerically the equation, the ωt_{max} value is calculated in function of the parameter values q and D, using ωt_{max} the peak value of the switch voltage value gain ($G_V(q, D)$)

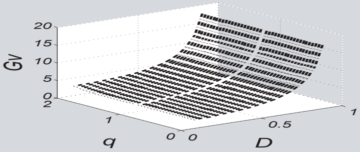

(a) 3D plot

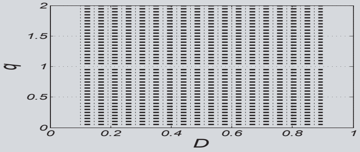

(b) q Vs. D

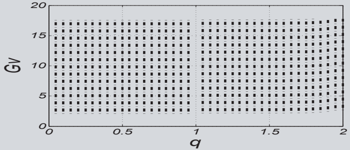

(c) G_V Vs. q

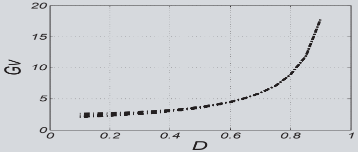

(d) G_V Vs. D

Peak voltage gain (G_V) for the ideal class-E PA

Curve fitting I

The gain was assumed as:

$$G_V a(D, q) = \frac{a}{1 - D};$$

where, a is a constraint value that minimizes the involved error. The goal function (S) was defined as:

$$S(a) = \sum_k \frac{{E_k}^2}{n}$$

where, n is the number of samples of the numerical solution. The fitting error was defined following the percentage least squares criteria as:

$$E_k = \frac{(G_{Va}(q_i, D_j) - G_V(q_i, D_j))}{G_V(q_i, D_j)}$$

Curve fitting II

RF Laboratory

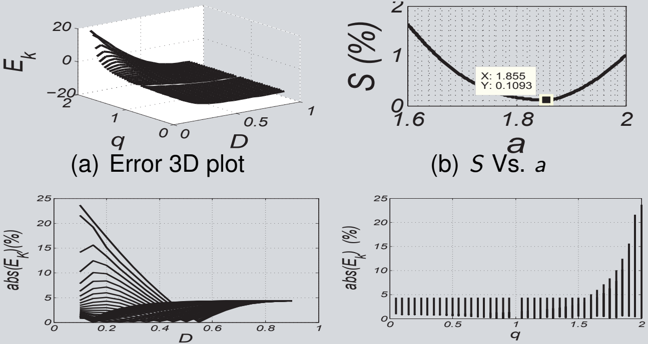

(a) Error 3D plot

(b) S Vs. a

(c) E_k Vs. D

(d) E_k Vs. q

Least squares fitting and error for a=1.8551

Curve fitting III

RF Laboratory

For $q > 1.65$, the values of either input parameters or circuit elements correspond to extreme values [13]. Hence considering $1.65 > q > 0.1$, and following a similar approach, the G_V can be expressed as:

$$G_V(D, q) = \frac{1.8208}{1 - D} \quad (19)$$

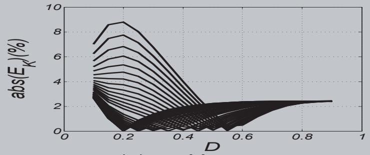

(a) E_k Vs. D

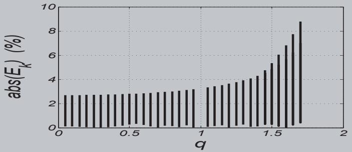

(b) E_k Vs. q

Least squares error for a=1.8208

Curve fitting for fixed D

In order to reduce the approximation error in the peak value prediction, for a fixed duty cycle ($D = D_x$), the approximative expression may be refined using a polynomial c(x) of degree n of the variable q that fits the data, in the least squares sense.

The gain was assumed as:

$$G_V a(D_x, q) = \frac{c(q)}{1 - D_x} = \frac{c_0 + c_1 q + \cdots + c_n q^n}{1 - D_x} \quad (20)$$

The optimum for n=2:

$$G_V a(D_x, q) = \frac{1.7613 + 0.0500q}{1 - D_x} \quad (21)$$

Curve fitting for D=50%

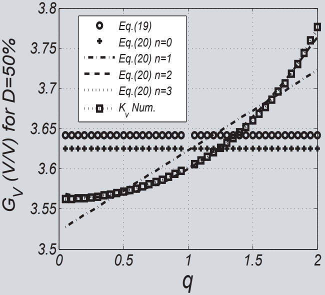

(a) G_V Vs. q

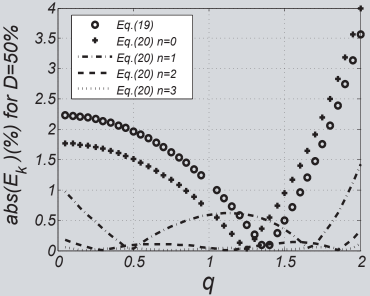

(b) E_k Vs. q

Polynomial fitting of G_V for D=50%

Simulated and Experimental Results

In order to verify (19), (21) and the numerical solution (Num), a PA was simulated following the specifications summarized in table, for experimental setup a fixed value of Q_L was used ($Q_L = 6$).

q	D (%)	f (MHz)	V_{CC} (V)	Q_L	R_L (Ω)
0.8,1.412,1.65	50	10,24	2	100,10,6	22

The simulation setup uses the harmonic balance simulation technique in the Advanced Design System (ADS®) software. Furthermore, the transistor is represented as a voltage controlled switch model, with ideal control signal (with 0 time transitions at a frequency f), an on resistance of 1 mΩ, and an open resistance of 100 GΩ. All the other circuit elements are simulated as ideal components.

Simulated Setup

q=0.8 QL=6

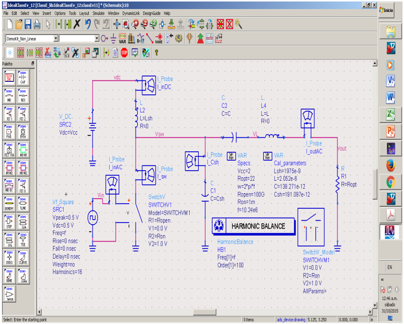

q=0.8 QL=6

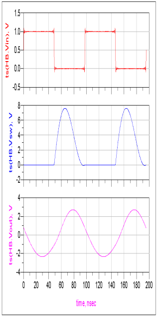

Eqn Pout=abs(0.5*real((HB.Vout)*conj(HB.I_outAC.i)))

Eqn Pout0=0.5*real(HB.Vout*conj(HB.I_outAC.i))

Eqn Pin=abs(0.5*real(HB.Vin*conj(HB.I_inAC.i)))

Eqn Poutdbm=10*log(Pout)+30

Eqn Pindbm=10*log(Pin)+30

Eqn Pdc=real(HB.I_inDC.i*HB.vdc)

Eqn PAE=100*(Pout[1]-Pin[0])/(Pdc[0])

Eqn Eff=100*Pout[1]/Pdc[0]

Pout[1]	Pdc[0]	Eff	PAE
0.144	0.145	99.332	99.332

Eqn Vmaxsw=max(ts(HB.Vsw))

Eqn VCC=real(HB.vdc[0])

Eqn IinDC=real(HB.I_inDC.i[0])

Eqn Vmax_Vcc=Vmaxsw/VCC

Eqn Rdc=mag(HB.vdc[0]/HB.I_inDC.i[0])

Vmaxsw	VCC	Vmax_Vcc	Rdc
7.620	2.000	3.810	27.671

Experimental Setup

The experimental results are taken from [13]

A discrete Class-E PAs were constructed with a transistor (MAX 2601), and discrete passive components. Further, the transistor gate was driven by a square wave signal from the signal source. The rise and fall time was chosen as 10 % of the period of the square signal (10.24 MHz).

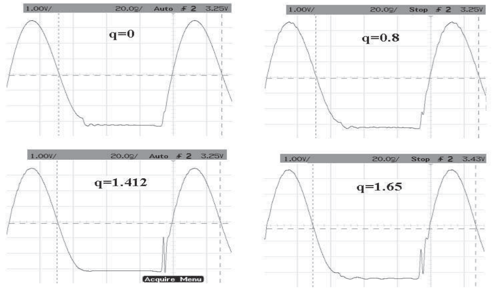

Experimental and Simulated Results

q	Parameter	Theoric			Sim. (QL=100)	Sim. (QL=10)	Sim. (QL=6)	Meas. (QL=6)
0.8	P_{out} (mW)	136.8			138.0	141.0	144.0	96.6
	P_{DC} (mW)	136.8			138.0	141.0	145.0	114.8
	Drain η (%)	100.0			99.9	99.8	99.3	84.1
	G_V (Num,Eq19,Eq21) (V/V)	3.59	3.64	3.60	3.60	3.72	3.81	3.35
	V_{S_M} (Num,Eq19,Eq21) (V)	7.17	7.28	7.21	7.20	7.44	7.62	6.70
	R_{DC} (Ω)	29.2			29.0	28.3	27.7	34.8
1.412	P_{out} (mW)	247.9			249.0	252.0	255.0	171.1
	P_{DC} (mW)	247.9			249.0	253.0	256.0	203.2
	Drain η (%)	100.0			99.9	99.8	99.6	84.2
	G_V (Num,Eq19,Eq21) (V/V)	3.65	3.64	3.66	3.66	3.72	3.77	3.33
	V_{S_M} (Num,Eq19,Eq21) (V)	7.29	7.28	7.33	7.32	7.44	7.55	6.65
	R_{DC} (Ω)	16.1			16.1	15.8	15.6	19.7
1.65	P_{out} (mW)	140.4			141.0	145.0	149	103.5
	P_{DC} (mW)	140.4			141.0	145.0	150	134.2
	Drain η (%)	100.0			99.9	99.7	99.1	77.1
	G_V (Num,Eq19,Eq21) (V/V)	3.69	3.64	3.69	3.70	3.83	3.93	3.45
	V_{S_M} (Num,Eq19,Eq21) (V)	7.37	7.28	7.38	7.40	7.65	7.86	6.90
	R_{DC} (Ω)	28.5			28.4	27.5	26.7	29.8

Modeling Error

Error (%)	G_V or V_{S_M} Num	Eq19	Eq21	RDC	q 0.80	1.412	1.65	QL 100	10	6
Mean	5.98	6.40	6.10	9.52	4.46	4.10	4.36	0.51	2.95	9.42
Max	9.68	9.52	10.20	18.02	16.06	18.02	7.36	1.55	4.83	18.02

- The predicted error involved in the expression analyzed (i.e. (19), (21) and Num is less than 20% including simulated and experimental results.

Modeling Error

Error (%)	G_V or V_{S_M} Num	Eq19	Eq21	RDC	q 0.80	1.412	1.65	QL 100	10	6
Mean	5.98	6.40	6.10	9.52	4.46	4.10	4.36	0.51	2.95	9.42
Max	9.68	9.52	10.20	18.02	16.06	18.02	7.36	1.55	4.83	18.02

- The predicted error involved in the expression analyzed (i.e. (19), (21) and Num is less than 20% including simulated and experimental results.
- The minimum error prediction of the G_V is achieved using (19), because the un-modeled dynamics (i.e. finite Q_L) increase the error of the numerical solution, as is clear from the increase of the error with a lower value of Q_L.

Modeling Error

Error (%)	G_V or V_{S_M} Num	Eq19	Eq21	RDC	q 0.80	1.412	1.65	QL 100	10	6
Mean	5.98	6.40	6.10	9.52	4.46	4.10	4.36	0.51	2.95	9.42
Max	9.68	9.52	10.20	18.02	16.06	18.02	7.36	1.55	4.83	18.02

- The predicted error involved in the expression analyzed (i.e. (19), (21) and Num is less than 20% including simulated and experimental results.
- The minimum error prediction of the G_V is achieved using (19), because the unmodeled dynamics (i.e. finite Q_L) increase the error of the numerical solution, as is clear from the increase of the error with a lower value of Q_L.

Conclusion

The equation (19) is a simple appropriate expression for modeling G_V.

Conclusions

- An analytical expression of the gain between the DC input voltage and the peak switch voltage on a ideal class-E power amplifier (PA) for a finite dc-feed inductance and ZVS and DZVS operation was presented.

Conclusions

- An analytical expression of the gain between the DC input voltage and the peak switch voltage on a ideal class-E power amplifier (PA) for a finite dc-feed inductance and ZVS and DZVS operation was presented.
- This expression was verified by the simulations, and was evaluated by experimental results (i.e at $f = 10.24$ MHz), with good agreement between the results and the predicted values.

Conclusions

- An analytical expression of the gain between the DC input voltage and the peak switch voltage on a ideal class-E power amplifier (PA) for a finite dc-feed inductance and ZVS and DZVS operation was presented.
- This expression was verified by the simulations, and was evaluated by experimental results (i.e at $f = 10.24$ MHz), with good agreement between the results and the predicted values.
- Considering the simulated and experimental results the maximum predicted error was 10,2%.

References I

[1] U. Nations, “World population prospects: The 2012 revision, highlights and advance tables (working paper no. esa/p/wp. 228),” 2013.

[2] E. Jovanov and A. Milenkovic, “Body area networks for ubiquitous healthcare applications: opportunities and challenges,” *Journal of medical systems*, vol. 35, no. 5, pp. 1245–1254, 2011.

[3] S. Movassaghi, M. Abolhasan, J. Lipman, D. Smith, and A. Jamalipour, “Wireless body area networks: A survey,” pp. 1–29, 2014, iD: 1.

[4] G. A. Rincon-Mora, “Powering microsystems with ambient energy.” CRC Press, 2013, pp. 1–30.

[5] F. Cabrera and F. Rangel de Sousa, “A 25-dbm 1-ghz power amplifier integrated in cmos 180nm for wireless power transferring,” in *Integrated Circuits and Systems Design, 2016.Proceedings*, 2016.

[6] J.-S. Paek and S. Hong, “A 29 dbm 70.7amplifier for pwm digitized polar transmitter,” *Microwave and Wireless Components Letters, IEEE*, vol. 20, no. 11, pp. 637–639, Nov 2010.

[7] W.-Y. Kim, H. S. Son, J. H. Kim, J. Y. Jang, I. Y. Oh, and C. S. Park, “A fully integrated triple-band cmos class-e power amplifier with a power cell resizing technique and a multi-tap transformer,” *Microwave and Wireless Components Letters, IEEE*, vol. 23, no. 12, pp. 659–661, Dec 2013.

[8] C. Yoo and Q. Huang, “A common-gate switched 0.9-w class-e power amplifier with 41vol. 36, no. 5, pp. 823–830, May 2001.

[9] N. Sokal and A. Mediano, “Redefining the optimum rf class-e switch-voltage waveform, to correct a long-used incorrect waveform,” in *IEEE MTT-S Int. Microwave Symp. Dig.*, June 2013, pp. 1–3.

References II

RF Laboratory

[10] R. Sadeghpour and A. Nabavi, “Design procedure of quasi-class-e power amplifier for low-breakdown-voltage devices,” *IEEE Trans. Circuits Syst. I, Reg. Papers*, vol. 61, no. 5, pp. 1416–1428, May 2014.

[11] A. Fajardo and F. Rangel de Sousa, “Integrated cmos class-e power amplifier for wireless power transfer,” presented at the IEEE Int. Symp. on Circuits and Systems, Montreal, Canada, 2016.

[12] M. Acar, A. Annema, and B. Nauta, “Analytical design equations for class-e power amplifiers,” *IEEE Trans. Circuits Syst. I, Reg. Papers*, vol. 54, no. 12, pp. 2706–2717, Dec 2007.

[13] ——, “Generalized design equations for class-e power amplifiers with finite dc feed inductance,” in *36th European Microwave Conference*, Sept 2006, pp. 1308–1311.

Obrigado

E-mail: fajardoa@javeriana.edu.co
Site: http://lrf.ufsc.br/

UNIVERSIDADE FEDERAL
DE SANTA CATARINA